engineering proceedings

MDPI

Proceeding Paper

On the Adaptive Numerical Solution to the Darcy–Forchheimer Model †

María González * and Hiram Varela *

Departamento de Matemáticas and CITIC, Universidade da Coruña, Campus de Elviña s/n, 15071 A Coruña, Spain

* Correspondence: maria.gonzalez.taboada@udc.es (M.G.); hiram.varela@udc.es (H.V.)

† Presented at the 4th XoveTIC Conference, A Coruña, Spain, 7–8 October 2021.

Abstract: We considered a primal-mixed method for the Darcy–Forchheimer boundary value problem. This model arises in fluid mechanics through porous media at high velocities. We developed an a posteriori error analysis of residual type and derived a simple a posteriori error indicator. We proved that this indicator is reliable and locally efficient. We show a numerical experiment that confirms the theoretical results.

Keywords: Darcy–Forchheimer; mixed finite element; a posteriori error estimates

Citation: González, M.; Varela, H. On the Adaptive Numerical Solution to the Darcy–Forchheimer Model. *Eng. Proc.* **2021**, *7*, 36. https://doi.org/10.3390/engproc2021007036

Academic Editors: Joaquim de Moura, Marco A. González, Javier Pereira and Manuel G. Penedo

Published: 18 October 2021

1. Introduction

The Darcy–Forchheimer model constitutes an improvement of the Darcy model which can be used when the velocity is high [1]. It is useful for simulating several physical phenomena, remarkably including fluid motion through porous media, as in petroleum reservoirs, water aquifers, blood in tissues or graphene nanoparticles through permeable materials. Let Ω be a bounded, simply connected domain in $\mathbb{R}^2$ with a Lipschitz-continuous boundary $\partial\Omega$. The problem reads as follows: given known functions $\mathbf{g}$ and f, find the velocity $\mathbf{u}$ and the pressure p such that

$$\left\{\begin{array}{rcll} \dfrac{\mu}{\rho}K^{-1}\mathbf{u}+\dfrac{\beta}{\rho}|\mathbf{u}|\mathbf{u}+\nabla p & = & \mathbf{g} & \text{in}\,\Omega, \\ \nabla\cdot\mathbf{u} & = & f & \text{in}\,\Omega, \\ \mathbf{u}\cdot\mathbf{n} & = & 0 & \text{on}\,\partial\Omega, \end{array}\right. \tag{1}$$

where μ is the dynamic viscosity, ρ denotes the fluid density, β is the *Forchheimer number* K denotes the permeability tensor, $\mathbf{g}$ represents gravity, f is compressibility, and $\mathbf{n}$ is the unit outward normal vector to $\partial\Omega$.

We make use of the finite element method to approximate the solution of problem (1). We present the approach by Girault and Wheeler [1], who introduced the primal formulation, in which the term $\nabla\cdot\mathbf{u}$ undergoes weakening by integration by parts. It is shown in [1] that problem (1) has a unique solution in the space $X\times M$, where $X:=[L^3(\Omega)]^2$ and $M:=W^{1,3/2}(\Omega)\cap L^2_0(\Omega)$ (we use the standard notations for Lebesgue and Sobolev spaces).

2. Discrete Problem

To pose a discrete problem, we can use a family $\{\mathcal{T}_h\}_{h>0}$ of conforming triangulations to divide the domain $\bar{\Omega}$ such that $\bar{\Omega}=\bigcup_{T\in\mathcal{T}_h}T$, $\forall h$, where $h>0$ represents the mesh size. Here we follow [2] and choose the following conforming discrete subspaces of X and M, respectively:

$$X_h := \left\{ \mathbf{v}_h \in [L^2(\Omega)]^2; \forall T \in \mathcal{T}_h, \mathbf{v}_h|_T \in [\mathbb{P}_0(T)]^2 \right\} \subset X,$$
$$M_h := Q_h^1 \cap L_0^2(\Omega) \subset M,$$

where $Q_h^1 := \left\{ q_h \in \mathcal{C}^0(\overline{\Omega}); \forall T \in \mathcal{T}_h, q_h|_T \in \mathbb{P}_1(T) \right\}$.

Then, the discrete problem consists in finding $(\mathbf{u}_h, p_h) \in X_h \times M_h$ such that

$$\left\{ \begin{array}{rcll} \displaystyle\int_\Omega \left(\frac{\mu}{\rho} K^{-1} \mathbf{u}_h + \frac{\beta}{\rho} |\mathbf{u}_h| \mathbf{u}_h \right) \cdot \mathbf{v}_h \, dx + \int_\Omega \nabla p_h \cdot \mathbf{v}_h \, dx & = & \displaystyle\int_\Omega \mathbf{g} \cdot \mathbf{v}_h \, dx, & \forall \mathbf{v}_h \in X_h, \\ \displaystyle\int_\Omega \nabla q_h \cdot \mathbf{u}_h \, dx & = & \displaystyle -\int_\Omega q_h f \, dx, & \forall q_h \in M_h. \end{array} \right. \tag{2}$$

It is shown in [2] that problem (2) has a unique solution and that the sequence $\{(\mathbf{u}_h, p_h)\}_h$ converges to the exact solution of problem (1) in $X \times M$. Furthermore, under additional regularity assumptions on the exact solution, some error estimates were derived in [2].

3. Novel Error Estimator and Adaptive Algorithm

We denote by $\mathcal{E}_\Omega$, $\mathcal{E}_{\partial\Omega}$ and $\mathcal{E}_T$, respectively, the sets of edges e belonging to the interior domain, the boundary and the element T; h_e denotes the length of a particular edge e; and h_T is the diameter of a given element T. We denote by $\mathbb{J}_e(v)$ the jump of v across the edge e in the direction of $\mathbf{n}_e$, a fixed normal vector to side e. Finally, we use the operator $\widetilde{\mathcal{A}}(\mathbf{u}_h, p_h) := \frac{\mu}{\rho} K^{-1} \mathbf{u}_h + \frac{\beta}{\rho} |\mathbf{u}_h| \mathbf{u}_h + \nabla p_h - \mathbf{g}$.

On every triangle $T \in \mathcal{T}_h$, we propose the following a posteriori error indicator:

$$\theta_T = \left(h_T^2 ||\widetilde{\mathcal{A}}(\mathbf{u}_h, p_h)||^2_{[L^2(T)]^2} + ||\nabla \cdot \mathbf{u}_h - f||^2_{L^2(T)} + \frac{1}{2} \sum_{e \in \mathcal{E}_\Omega \cap \partial T} h_T^{-1} ||\mathbb{J}_e(\mathbf{u}_h \cdot \mathbf{n})||^2_{L^2(e)} + \sum_{e \in \mathcal{E}_{\partial\Omega} \cap \partial T} h_T^{-1} ||\mathbf{u}_h \cdot \mathbf{n}||^2_{L^2(e)} \right)^{1/2}$$

We also define the global a posteriori error indicator $\theta := \left(\sum_{T \in \mathcal{T}_h} \theta_T^2 \right)^{1/2}$.

Theorem 1. *For the primal-mixed method (2), there exists a positive constant C_1, independent of h, and a positive constant C_2, independent of h and T, such that*

$$||(\mathbf{u} - \mathbf{u}_h, p - p_h)||_{X \times M} \le C_1 \theta,$$
$$\theta_T \le C_2 ||(\mathbf{u} - \mathbf{u}_h, p - p_h)||_{[L^3(w_T)]^2 \times W^{1,3/2}(w_T)}, \quad \forall T \in \mathcal{T}_h,$$

where $w_T = \bigcup_{\mathcal{E}_T \cap \mathcal{E}_{T'} \neq \varnothing} T'$.

We propose an adaptive algorithm based on the a posteriori error indicator θ. Given an initial mesh, we follow the iterative procedure described in Figure 1. Each new mesh is generated as suggested in [3].

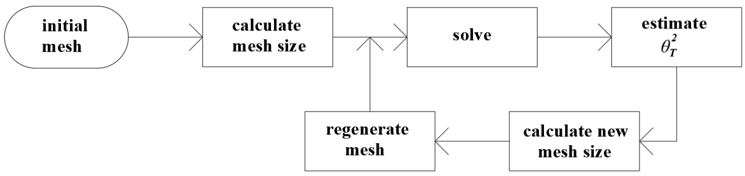

Figure 1. Adaptive algorithm flux diagram.

4. Numerical Experiment

We performed several simulations in FreeFem++ [4], validating the theoretical results. Here we select an example on an L-shaped domain, $\Omega = (-1,1)^2 \backslash [0,1]^2$, and focus on the data f and $\mathbf{g}$ so that the exact solution is

$$p(x,y) = \frac{1}{x-1.1}, \quad \mathbf{u}(x,y) = \begin{pmatrix} \exp(x)\sin(y) \\ \exp(x)\cos(y) \end{pmatrix}. \tag{3}$$

Thus the solution has a singularity in pressure close to the line $x = 1$. Figure 2 shows the mesh refinement by the adaptive algorithm. Figure 3, bottom, represents the evolution with respect to degrees of freedom (DOF) of error and indicator; on the right, we can observe the evolution of the efficiency index with DOF.

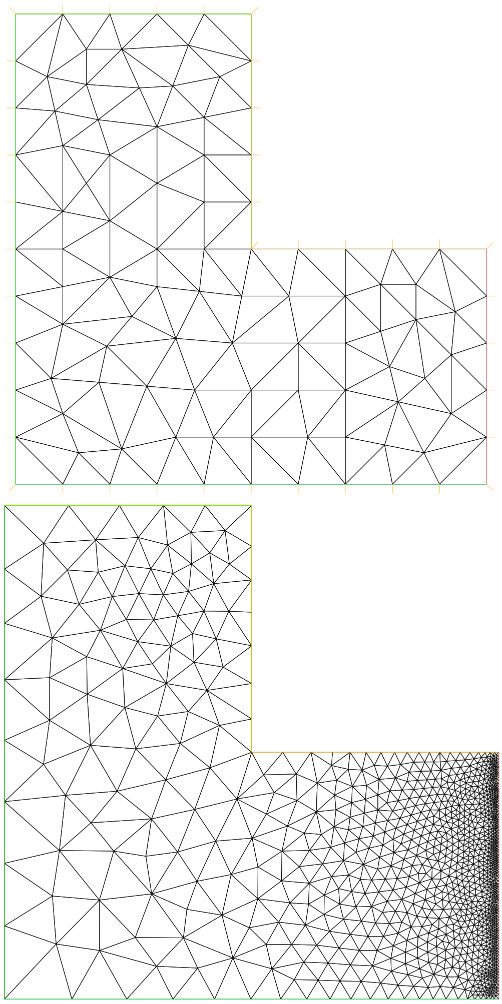

Figure 2. Example 1. Initial mesh (270 DOF) on the (**top**); intermediate adapted mesh with 1512 DOF on the (**bottom**).

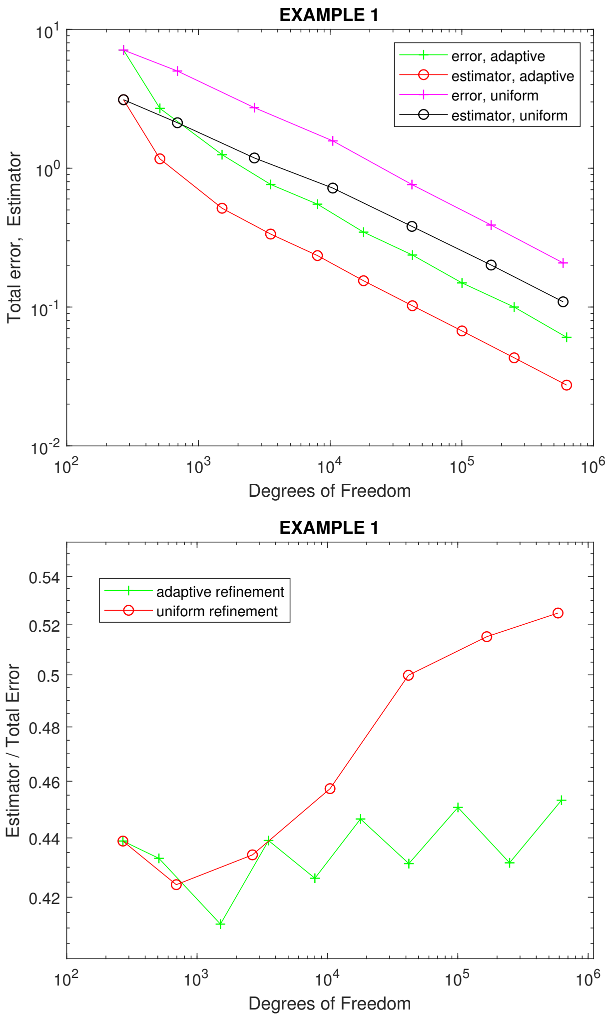

Figure 3. Example 1. (**Top**): Error and indicator evolution vs. DOF. (**Bottom**): Efficiency index vs. DOF.

5. Discussion

The adaptive algorithm was tested on an example with a singularity. From Figure 2 we can observe that the algorithm refined the mesh near the singularity, as expected. Since it is an academic example with a known solution, we could compute the exact error. The graphs in Figure 3 confirm that the error was lower for the adaptive refinement. Additionally, since the exact error and estimator followed close to parallel lines, we confirm that the indicator gives a consistent measure of the error. This could also be checked by the efficiency index, which is the ratio of indicator to exact total error.

Funding: The authors acknowledge the support of CITIC (FEDER Program and grant ED431G 2019/01). The research of M.G. is partially supported by Xunta de Galicia Grant GRC ED431C 2018-033. The research of H.V. is partially supported by Ministerio de Educación grant FPU18/06125.

Institutional Review Board Statement: Not applicable.

Informed Consent Statement: Not applicable.

Conflicts of Interest: The authors declare no conflict of interest.

References

1. Girault, V.; Wheeler, M.F. Numerical Discretization of a Darcy-Forchheimer Model. *Numer. Math.* **2008**, *110*, 161–198. [CrossRef]
2. Salas, J.J.; López, H.; Molina, B. An analysis of a mixed finite element method for a Darcy-Forchheimer model. *Math. Comput. Model.* **2013**, *57*, 2325–2338. [CrossRef]
3. Borouchaki, H.; Hecht, F.; Frey, P. Mesh gradation control. *Int. J. Numer. Meth. Eng.* **1998**, *43*, 1143–1165. [CrossRef]
4. Hetch, F. FreeFEM Documentation, Release 4.6. 2020. Available online: https://doc.freefem.org/pdf/FreeFEM-documentation.pdf (accessed on 13 October 2021).